AD-A032 722 CORNELL UNIV ITHACA N Y F/G 20/3
NOISE LIMITATIONS OF RF SQUIDS.(U)
OCT 76 R A BUHRMAN
UNCLASSIFIED TR-4 N00014-76-C-0526
NL

1 OF 1
AD A032722

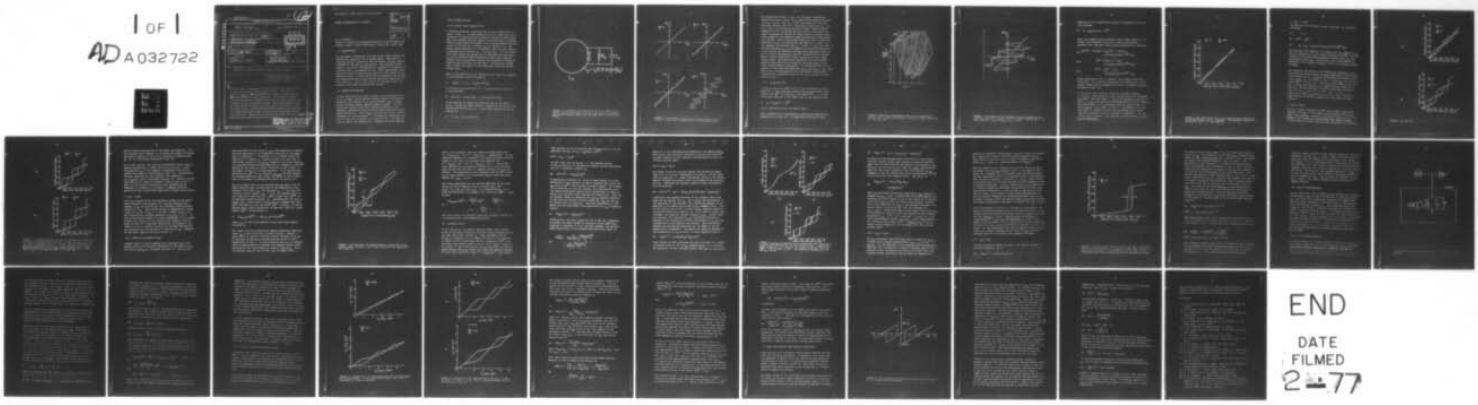

END
DATE FILMED
2-77

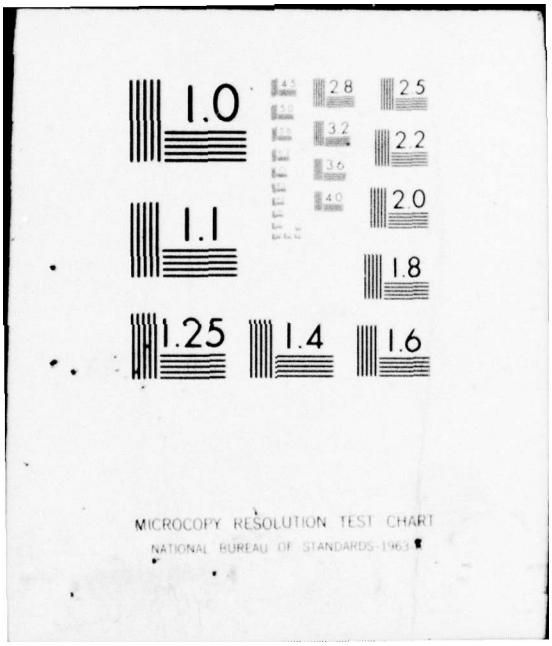
1.0
1.1
1.25
1.4
1.6
1.8
2.0
2.2
2.5
2.8
3.2
3.6
4.0
MICROCOPY RESOLUTION TEST CHART
NATIONAL BUREAU OF STANDARDS-1963

UNCLASSIFIED
Security Classification

(12)

AD A032722

## DOCUMENT CONTROL DATA - R & D

*(Security classification of title, body of abstract and indexing annotation must be entered when the overall report is classified)*

1. ORIGINATING ACTIVITY (Corporate author)
Cornell University
Ithaca, New York 14853

2a. REPORT SECURITY CLASSIFICATION
Unclassified

2b. GROUP

3. REPORT TITLE
(6) NOISE LIMITATIONS OF rf SQUIDS.

DDC
RECEIVED
NOV 26 1976
B

4. DESCRIPTIVE NOTES (Type of report and inclusive dates)
(9) Technical Report

5. AUTHOR(S) (First name, middle initial, last name)
(10) Robert A. Buhrman

| 6. REPORT DATE | 7a. TOTAL NO. OF PAGES | 7b. NO. OF REFS |
|---|---|---|
| (11) 5 October 1976 | (12) 38 p. | 19 |

| 8a. CONTRACT OR GRANT NO. | 9a. ORIGINATOR'S REPORT NUMBER(S) |
|---|---|
| NR319-096 | Technical Report #4 |
| b. PROJECT NO. (15) N00014-76-C-0526 | (14) TR-4 |
| c. | 9b. OTHER REPORT NO(S) (Any other numbers that may be assigned this report) |
| d. | |

10. DISTRIBUTION STATEMENT
Approved for public release; distribution unlimited

| 11. SUPPLEMENTARY NOTES | 12. SPONSORING MILITARY ACTIVITY |
|---|---|
| | Office of Naval Research<br>Electronics Program Office<br>Arlington, VA 22217 |

13. ABSTRACT

In this paper a discussion is given of the noise sources and sensitivity limits of the rf biased SQUID. Both the low critical current inductive and the higher critical current hysteretic devices are considered. The intrinsic SQUID noise is treated by considering the internal flux response of a SQUID ring to an applied rf flux. While approximate, this approach yields the most direct picture of the nature of the intrinsic noise. Circuit optimization procedures for maximizing SQUID performance under various operating conditions are also outlined. Finally the effects of non-ideal weak link behavior upon SQUID operation are treated.

098 550



DD FORM 1 NOV 65 1473

UNCLASSIFIED
Security Classification

[Proceedings, IC SQUID, Berlin, 5-8 October 1976]



# NOISE LIMITATIONS OF rf SQUIDs

R. A. Buhrman
School of Applied and Engineering Physics, and The Materials Science Center, Cornell University, Ithaca, NY 14853, USA

## I. INTRODUCTION

In this paper a discussion is given of the noise sources and sensitivity limits of the rf biased SQUID. Both the low critical current "inductive" and the higher critical current "hysteretic" devices are considered. The intrinsic SQUID noise is treated by considering the internal flux response of a SQUID ring to an applied rf flux. While approximate, this approach yields the most direct picture of the nature of the intrinsic noise. Circuit optimization procedures for maximizing SQUID performance under various operating conditions are also outlined. Finally the effects of non-ideal weak link behavior upon SQUID operation are treated.

## II. SQUID RING RESPONSE

A basic understanding of the origins of the intrinsic noise of an rf SQUID can be obtained through study of the general nature of the response of an isolated SQUID ring to quasi-static and time varying applied magnetic fields. In this section we briefly sketch the essential details of this response, emphasizing those features which ultimately affect SQUID sensitivity. More complete discussions can be found elsewhere in the literature.[1-7] We begin by considering the case of very low frequency or dc applied flux. The general case of SQUID ring response to a combined rf and dc applied

flux is then treated.

## II.1. Quasi-Static Applied Flux

A standard schematic representation of an rf SQUID ring is shown in Fig. 1. A superconducting ring of inductance $L_s$ is closed by a superconducting Josephson junction or weak link. The usual shunted junction model of the weak link is assumed, where a superconducting element with a current-phase relation $i_c f(\theta)$ is shunted by a resistor $R_s$ and capacitor $C_s$. For proper SQUID operation it is necessary that the weak link be overdamped which requires $C_s < (\phi_o/2\pi i_c)/R_s^2$. In the discussion that follows we assume this is the case and that hence $C_s$ can be neglected when determining SQUID ring response. Ideally the current-phase relation is sinusoidal although in practice this is often not the case.[7] Here we will assume $f(\theta) = \sin\theta$; the effect of non-sinusoidal $f(\theta)$ will be discussed later.

When an external flux $\phi_x$ is applied to the ring, the response of the internal flux $\phi$ is given by

$$1) \quad L_s\dot{\phi}/R_s + \phi = \phi_x - L_s i_c \sin(2\pi\phi/\phi_o) \quad .$$

As discussed by Kurkijärvi[8] Eq. (1) describes the motion of $\phi$ in the potential

$$2) \quad U(\phi,\phi_x) = (\phi-\phi_x)^2/2L_s - (\phi_o/2\pi) i_c \cos(2\pi\phi/\phi_o) \quad .$$

In the absence of thermal fluctuations and in the limit $\dot{\phi}_x/\phi_o << R_s/L_s$ the total current i flowing in the ring is the equilibrium supercurrent $i_s$. Under these conditions Eq. (1) reduces to

$$3) \quad \phi = \phi_x - L_s i_c \sin(2\pi\phi/\phi_o) \quad .$$

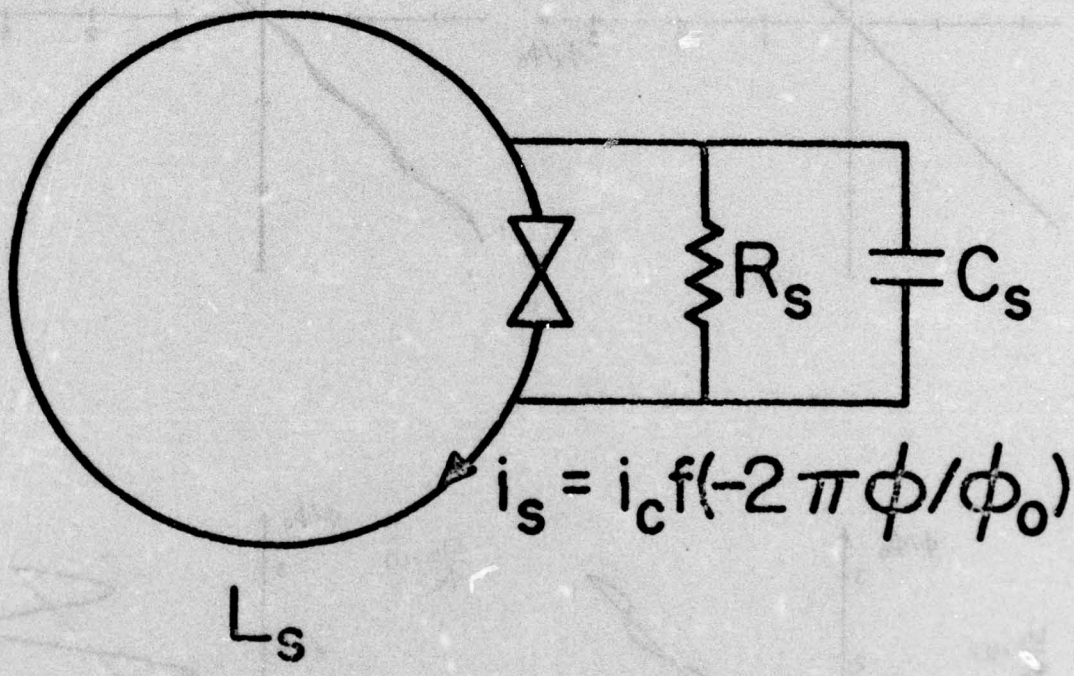


FIGURE 1. A schematic representation of an rf SQUID ring. Ideally the current-phase relation $f(-2\pi\phi/\phi_o)$ is sinusoidal and $C_s$ sufficiently small that the weak link is very overdamped.

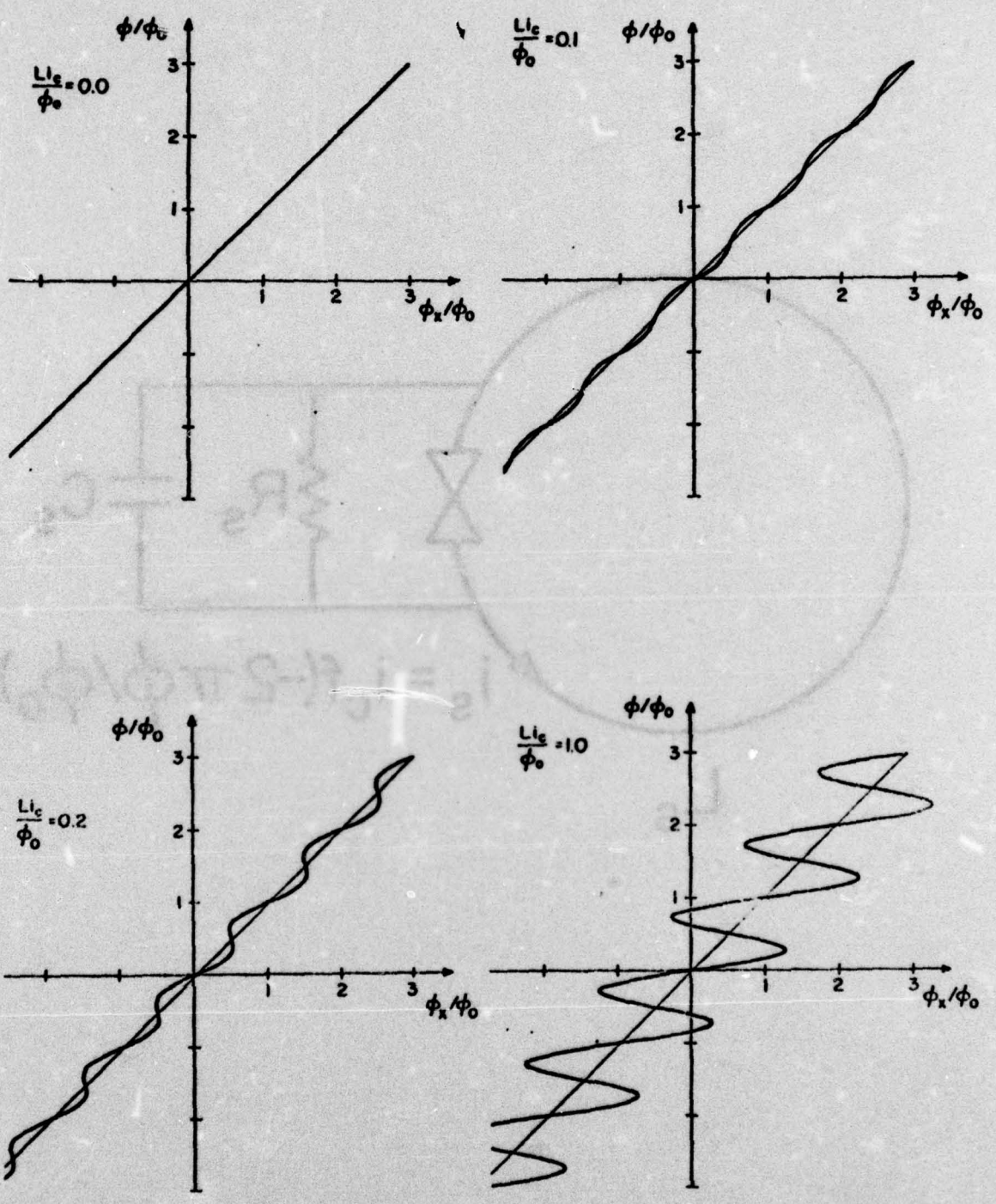


FIGURE 2. Quasi-static internal flux versus applied flux response curves for various values of critical currents.

As illustrated in Fig. 2, Eq. (3) in general describes a snake-like curve in the $\phi$ vs $\phi_x$ plane which becomes reentrant for $Li_c \geq \phi_o/2\pi$. For $Li_c < \phi_o/2\pi$ the system has only one potential minimum and $\phi$ is a continuous function of $\phi_x$. For $Li_c \geq \phi_o/2\pi$ the system has multiple fluxoid quantum states. Segments of $\phi$ vs $\phi_x$ curves such as in Fig. 2 with positive slope correspond to regions of local potential minima, while those segments with negative slope correspond to local potential maxima. This is shown most clearly in Fig. 3 where the potential $U(\phi,\phi_x)$ is plotted for the case $Li_c = 2.0\phi_o$. If, for example, we initially set $\phi_x = 0$ and $\phi = -1\phi_o$ as in Fig. 3 and then increase $\phi_x$, in the absence of thermal fluctuations $\phi$ will follow the potential minimum along the curve given by Eq. (3) until the potential barrier vanishes and the system makes a rapid transition in time $\sim L_s/R_s$ to the next lower energy state. The system will remain in this new fluxoid quantum state until $\phi_x$ is varied to the point where a new lower energy state is accessible. If an oscillatory flux is applied to the ring with amplitude $\geq \phi_{xc}$, where $\phi_{xc} \simeq Li_c + \phi_o/4$ and is the critical applied flux, the system will follow a discontinuous, hysteretic path in the $\phi$ vs $\phi_x$ plane as indicated in Fig. 4.

## II.2. rf Applied Flux

In general when the SQUID ring is to be operated as a flux detector, a high frequency biasing flux $\phi_{xm}\sin\omega t$ and a "dc" signal flux $\phi_x^{(dc)}$ is applied to the SQUID ring. It is the non-linear response of the SQUID ring to this applied flux

$$\phi_x = \phi_{xm}\sin\omega t + \phi_x^{(dc)} \quad , \tag{4}$$

which ultimately yields the SQUID signal.

This response can be determined by solving the equation of motion given by Eq. (3). An approximate solution can be

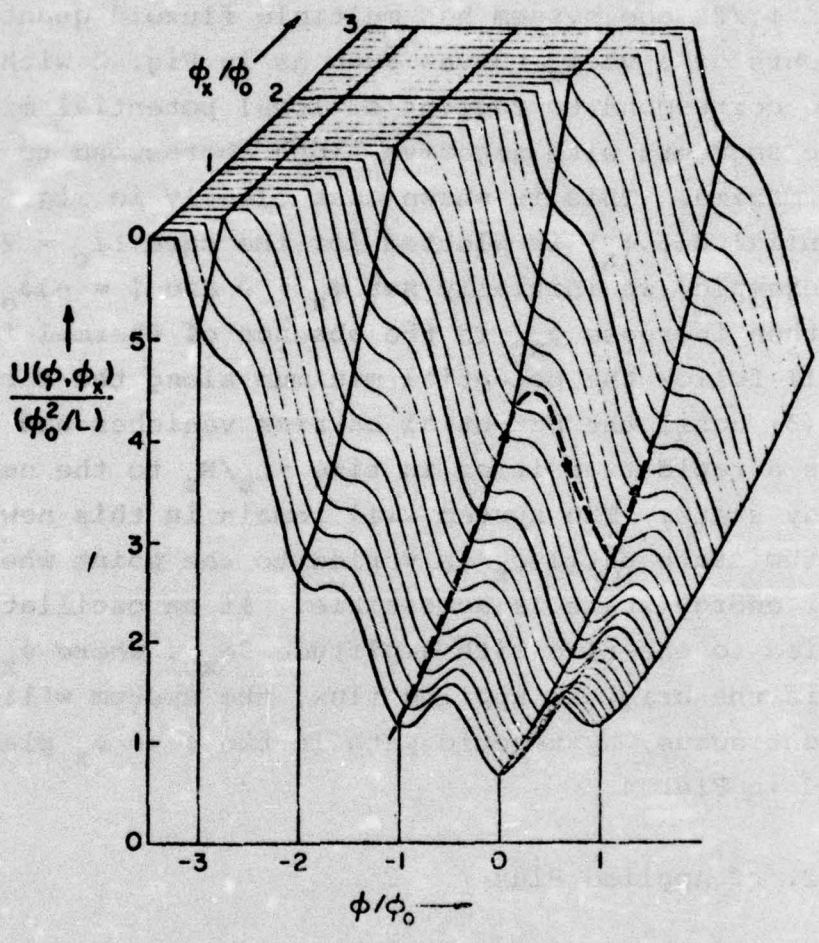


**FIGURE 3. Motion of the applied flux $\phi$ in the potential $U(\phi,\phi_x)$ for a slowly increasing $\phi_x$ and $L_s i_c = 2\phi_o$. Initially $\phi = -\phi_o$, $\phi_x = 0$.**

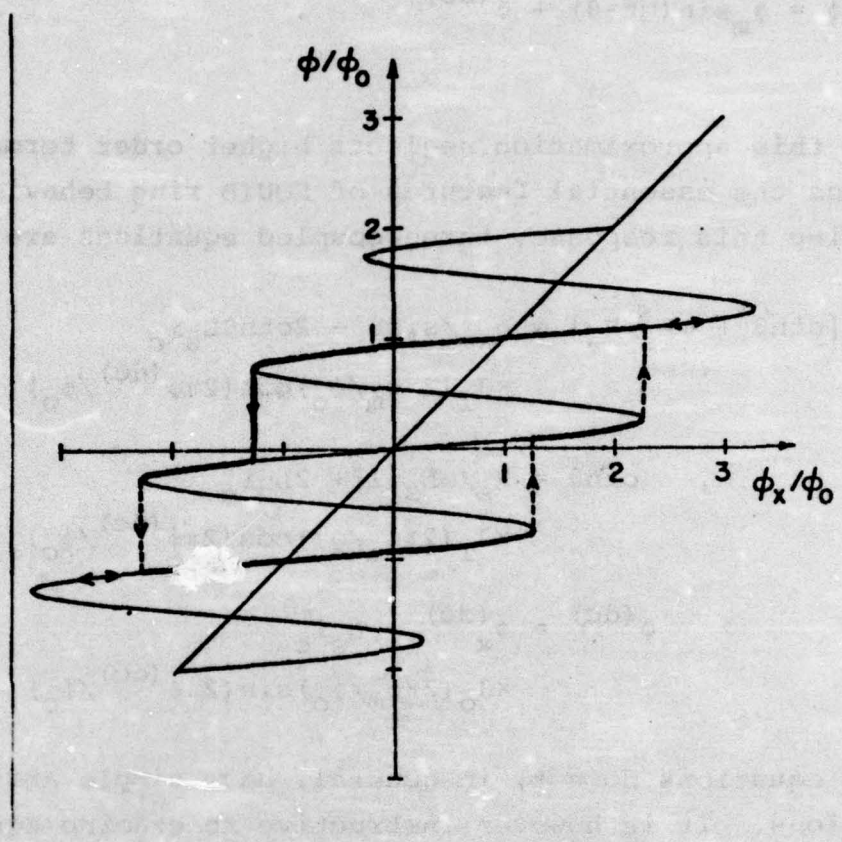


**FIGURE 4. An example of the hysteretic path followed by $\phi$ in the $\phi$-$\phi_x$ plane for a slowly varying periodic applied flux. In this case the critical current $L_s i_c \doteq 2\phi_0$.**

obtained in a straightforward manner by assuming an internal flux response

$$5) \quad \phi = \phi_m \sin(\omega t - \theta) + \phi^{(dc)} \quad .$$

While this approximation neglects higher order terms in $\omega$ it retains the essential features of SQUID ring behavior. Assuming this response, three coupled equations are obtained:

$$6a) \quad \phi_m[\mathrm{ctn}\theta + \omega L_s/R_s] = \phi_{xm}/\sin\theta - 2\mathrm{ctn}\theta L_s i_c \times J_1(2\pi\phi_m/\phi_o)\cos(2\pi\phi^{(dc)}/\phi_o)$$

$$6b) \quad \mathrm{ctn}\theta = R_s/\omega L_s[1 + 2L_s i_c \times J_1(2\pi\phi_m/\phi_o)\cos(2\pi\phi^{(dc)}/\phi_o)]$$

$$6c) \quad \phi^{(dc)} = \phi_x^{(dc)} - L_s i_c \times J_o(2\pi\phi_m/\phi_o)\sin(2\pi\phi^{(dc)}/\phi_o) \quad .$$

These equations do not, in general, have simple analytical solutions. It is however instructive to examine Eqs. (6) in various limits and to compare the results to complete digital solutions of Eq. (1).

In the usual case of SQUID operation the bias frequency $\omega << R_s/L_s$. This paper will only consider this low frequency situation. The case where $\omega \gtrsim R_s/L_s$ is discussed elsewhere.[9] When $\omega << R_s/L_s$ the internal flux response to $\phi_{xm}\sin\omega t$ follows the quasi-static $\phi$ vs $\phi_x$ response curve as given by Eq. (3) and as shown, for example, in Fig. 2. The effect of the dc flux $\phi_x^{(dc)}$ is simply to shift the equilibrium point about which the internal flux is modulated at frequency $\omega$. In discussing this response, three separate critical current regimes can be considered:

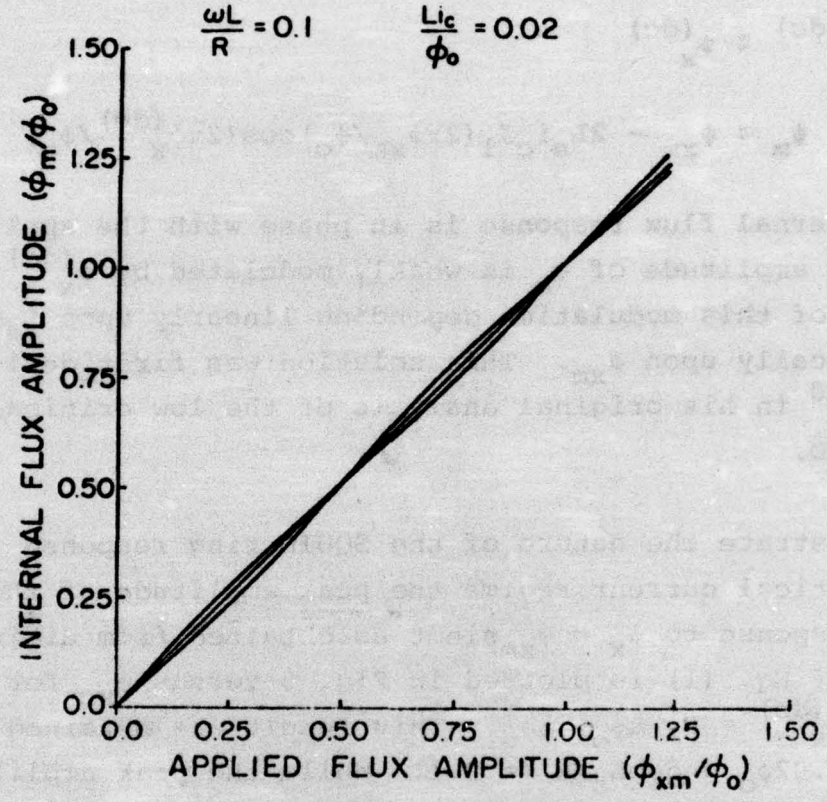


FIGURE 5. The peak amplitude of the internal flux response $\phi_m$ to an applied rf flux $\phi_x = \phi_{xm}\sin\omega t$. The response function is plotted for $\phi_x^{(dc)} = 0$, $\frac{1}{4}\phi_o$ and $\frac{1}{2}\phi_o$.

1. $L_s i_c \ll \phi_o/2\pi$

In this very low critical current limit Eqs. (6) yield the solutions

7a) $$\theta \simeq 0$$

7b) $$\phi^{(dc)} \simeq \phi_x^{(dc)}$$

7c) $$\phi_m \simeq \phi_{xm} - 2L_s i_c J_1(2\pi\phi_{xm}/\phi_o)\cos(2\pi\phi_x^{(dc)}/\phi_o) \quad .$$

The internal flux response is in phase with the applied flux and the amplitude of $\phi_m$ is weakly modulated by $\phi_x^{(dc)}$; the magnitude of this modulation depending linearly upon $L_s i_c$ and periodically upon $\phi_{xm}$. This solution was first derived by Hansma[10] in his original analysis of the low critical current rf SQUID.

To illustrate the nature of the SQUID ring response in this low critical current regime the peak amplitude of the internal flux response to $\phi_x = \phi_{xm}\sin\omega t$ as obtained from digital solutions of Eq. (1) is plotted in Fig. 5 versus $\phi_{xm}$ for the three cases $\phi_x^{(dc)} = 0$, $\frac{1}{4}\phi_o$, $\frac{1}{2}\phi_o$. This result was obtained assuming $Li_c = 0.02\phi_o$ and $\omega L_s/R_s = 0.1$. While the peak amplitude of the internal flux has both a slightly different periodicity than does $\phi_m$, as given by Eq. (7c), and a somewhat larger amplitude at high $\phi_{xm}$ drive levels, Fig. 5 does indicate the basic nature of the ring response for very small critical current.

2. $L_s i_c \lesssim \phi_o/2\pi$

As $L_s i_c \to \phi_o/2\pi$ screening currents in the SQUID ring become important and Eqs. (7) no longer satisfactorily explain the SQUID ring response. Recently Soerensen,[11] Erne et al.[12] and Hansma et al.[13] have all investigated this regime through various analytical means and have been successful in obtaining

(a)

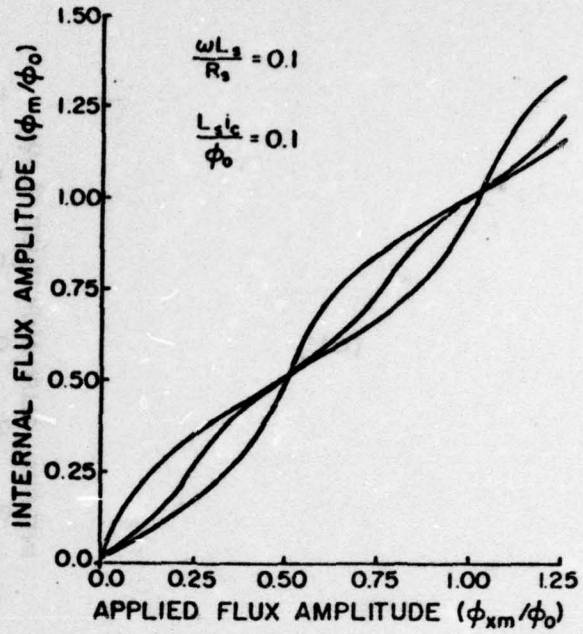


(b)

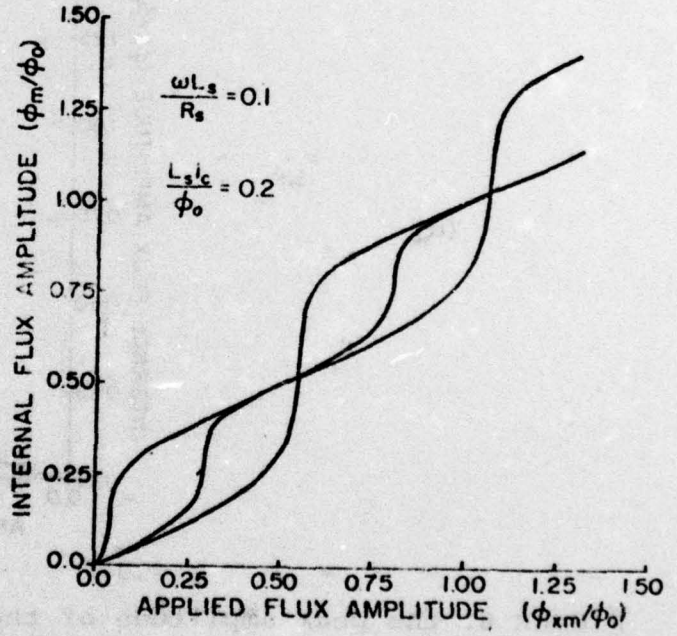


FIGURE 6 (a) and (b).

(c)

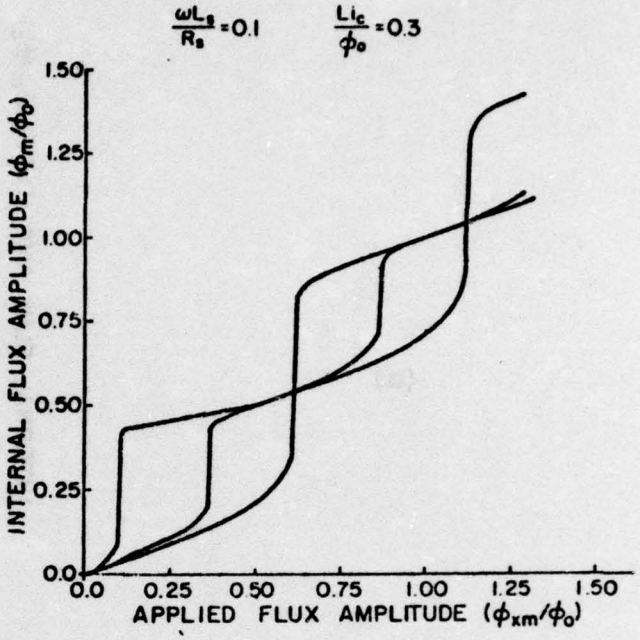


(d)

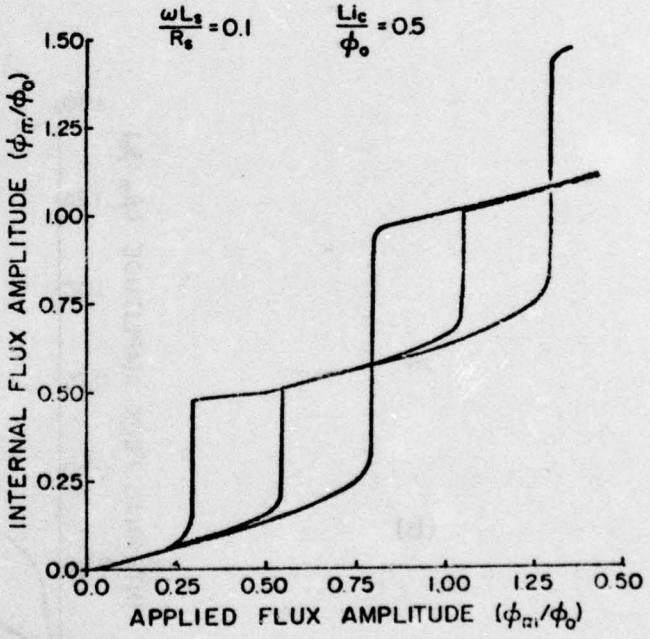


FIGURE 6. the peak amplitude of the rf response to the applied rf flux $\phi_x = \phi_{xm}\sin\omega t$ for (a) $L_s i_c = 0.1\phi_o$, (b) $L_s i_c = 0.2\phi_o$, (c) $L_s i_c = 0.3\phi_o$ and (d) $L_s i_c = 0.5\phi_o$. Due to the relatively high drive frequency $\omega L_s/R_s \approx 0.1$, the discontinuous regime actually begins at $L_s i_c \approx 0.2\phi_o$ rather than at $L_s i_c = \phi_o/2\pi$. The curves are plotted for $\phi_x^{(dc)} = 0$, $\frac{1}{4}\phi_o$, $\frac{1}{2}\phi_o$.

quite accurate descriptions of the SQUID ring behavior. For our purposes here, however, it is sufficient simply to discuss the general aspects of the $\phi$ vs $\phi_x$ response as deduced from Eq. (6) or from digital solutions to Eq. (1).

It is seen from Eq. (6b) that for sufficiently small $\omega L_s/R_s$ $\phi$ remains essentially in phase with $\phi_x$ for all $L_s i_c < \phi_o/2\pi$. The amplitude $\phi_m$ of the response at frequency $\omega$ can be obtained from numerical evaluations of Eqs. (6). Alternatively, the peak amplitude of this internal flux response to $\phi_x = \phi_{xm}\sin\omega t$ can be calculated from Eq. (1). Results of such calculations are shown for several values of $L_s i_c$ in Fig. 6. Again the distinction between the peak response and the component at frequency $\omega$ is slight: a somewhat different periodicity and a diminishing amplitude at higher drive levels.

3. $L_s i_c > \phi_o/2\pi$

Once $L_s i_c$ exceeds $\phi_o/2\pi$, the hysteretic nature of the quasi-static internal flux response to a periodic applied flux results in $\phi_m$, as given by Eq. (6), becoming a discontinuous function of $\phi_{xm}$. (This effect occurs at progressively larger values of $L_s i_c$ as $\omega L_s/R_s \to 1$. In Fig. 6 where $\omega L_s/R_s = 0.1$, the discontinuous response commences at $L_s i_c/\phi_o \simeq 0.2$.[9]) In this discontinuous regime it is most appropriate not to pursue further the analysis of the internal flux response from the point of view of a sinusoidal oscillation at frequency $\omega$ but rather to rely on digital solutions of the peak amplitude of the internal flux oscillation as a function of $\phi_{xm}$. Examples of this peak response are given in Fig. 6.

## II.3. Effect of dc Applied Flux

A major effect of the dc applied flux upon the $\phi$-$\phi_x$ rf response curve is the periodic modulation of the values of $\phi_{xm}$ for which $d\phi_m/d\phi_{xm}$ is a maximum (see Fig. 6). This is the

case regardless of the value of $L_s i_c$ and regardless of whether the peak amplitude of the response is detected on the component at frequency $\omega$. In general, in an rf SQUID system the SQUID ring is coupled to a biasing circuit in such a way so that those regions of the $\phi_m$-$\phi_{xm}$ response curve where $d\phi_m/d\phi_{xm}$ is a maximum present maximum opposition to changes in the flux applied by the biasing circuit, resulting in the "steps" in the SQUID circuit rf I-V characteristic. It is the periodic modulation by $\phi_x^{(dc)}$ of the location $\phi_{xm,max}$ of these regions of maximum opposition that yields the signal in the rf SQUID. This is discussed in somewhat more detail in section IV.

Thus the signal that can be obtained from the SQUID ring depends directly upon the amplitude of the modulation of the response curve about $\phi_{xm}$, for constant $\phi_m$. In the very low critical current regime, $L_s i_c << \phi_o/2\pi$, the maximum value of this modulation amplitude for a small signal flux $\delta\phi_x^{(dc)}$ can be obtained directly from Eq. (7). Assuming that the ring is biased near a point where $J_1(2\pi\phi_{xm}/\phi_o)$ is a maximum and that $\phi_x^{(dc)}$ has been set near the value, $\phi_x^{(dc)} = (n+\frac{1}{4})\phi_o$, for which maximum small signal sensitivity is obtained, then for a small signal $\delta\phi_x^{(dc)}$ the modulation is

$$8) \quad \delta\phi_{xm,max}(\delta\phi_x^{(dc)}) \simeq 2L_s i_c J_{1,m}(2\pi/\phi_o)\delta\phi_x^{(dc)}$$

where $J_{1,m}$ is the first maximum of the first order Bessel function $J_1$.

For larger critical currents the maximum modulation amplitude about $\phi_{xm}$ is more difficult to obtain exactly. However a value which is correct to within a factor of order unity can be obtained by employing the approximation which is shown graphically in Fig. 7. In this situation the $\phi$-$\phi_x$ rf response curve is approximated by straight line segments whose slopes are equal to the local minima and maxima of $d\phi_m/d\phi_{xm}$. If it is the peak value of the rf flux, such as shown in Fig. 7,

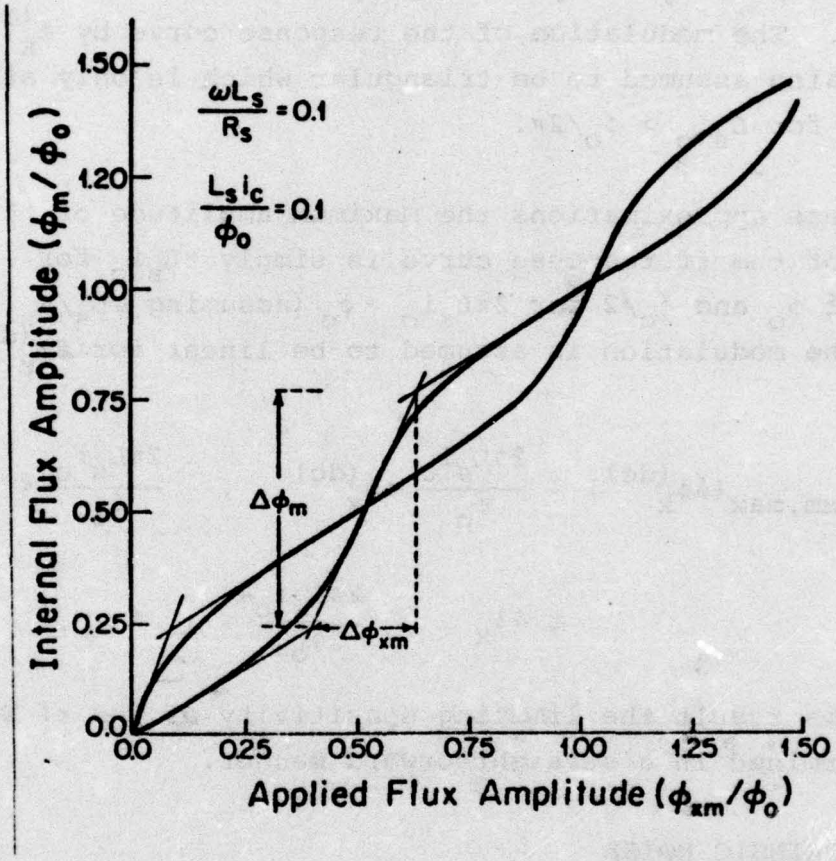


**FIGURE 7. The straight line approximation to the $\phi$-$\phi_x$ rf response curve. As $L_s i_c \to \phi_o/2\pi$ the accuracy of the approximation improves.**

which is of interest, then the values of these slopes are $(1 + 2\pi L_s i_c/\phi_o)^{-1}$ and $(1 - 2\pi L_s i_c/\phi_o)^{-1}$ respectively. If the response component at frequency $\omega$ is being considered then the slopes of the first two straight line segments are $[1 + 2L_s i_c J_1'(0)]^{-1}$ and $[1 - 2L_s i_c J_1'(3.7)]^{-1}$. The differences between the two cases are slight and in the discussion that follows only the peak rf response function will be considered. The modulation of the response curve by $\phi_x^{(dc)}$ about $\phi_{xm}$ is also assumed to be triangular which is only strictly correct for $L_s i_c > \phi_o/2\pi$.

With these approximations the maximum amplitude of the modulation of the rf response curve is simply $\pi L_s i_c$ for $2\pi L_s i_c \leq \phi_o$ and $\phi_o/2$ for $2\pi L_s i_c > \phi_o$ (assuming $\omega L_s/R_s << 1$). Since the modulation is assumed to be linear for $\delta\phi_x^{(dc)} < \phi_o/2$ we have

$$\delta\phi_{xm,max}(\delta\phi_x^{(dc)}) \simeq \frac{2\pi L_s i_c}{\phi_o}\,\delta\phi_x^{(dc)} \quad , \quad \frac{2\pi L_s i_c}{\phi_o} < 1$$

9)

$$\simeq \delta\phi_x \quad , \quad \frac{2\pi L_s i_c}{\phi_o} > 1 \quad .$$

With this result the limiting sensitivity of the rf SQUID can be determined in a straightforward manner.

## III. INTRINSIC NOISE

In the context of the shunted junction model, the intrinsic noise of the SQUID originates with the current fluctuations in the weak link shunt resistor $R_s$. When the SQUID ring is biased at frequency $\omega$ it is simply the ratio of its response to these current fluctuations and its response to $\phi_x^{(dc)}$ that determines the maximum sensitivity of the rf SQUID. Formally, the effect of these fluctuations can be determined by adding a noise current term $L_s i_N$ to Eq. (1), where the spectral density of this noise current is $\langle i_N^2(\nu)\rangle^{\frac{1}{2}} = (4k_B T_s/R_s)^{\frac{1}{2}}$. The problem

then becomes one of calculating the fluctuations of $\phi$ in the potential $U(\phi,\phi_x)$ for $\phi_x = \phi_{xm}\sin\omega t + \phi_x^{(dc)}$.

III.1. $L_s i_c << \phi_o/2\pi$

In this limit and for $\omega L_s/R_s << 1$ the problem reduces to the calculation of the spectral density of the fluctuating flux of a classical inductor $L_s$.

10) $$\langle\delta\phi^2(\nu)^{\frac{1}{2}}\rangle = (4k_B T_s L_s^2/R_s)^{\frac{1}{2}} .$$

As mentioned in Section II, in an rf SQUID system it is the modulation of the location of the rf response curve about the $\phi_{xm}$ axis by $\phi_x^{(dc)}$ that provides the SQUID signal. As a result it is necessary to cast the internal flux fluctuations into the form of equivalent applied flux fluctuations in order to obtain the intrinsic noise limited flux sensitivity. This can be achieved simply by employing the $\phi_m$-$\phi_{xm}$ response function. In the very low critical current regime $\phi_m \simeq \phi_{xm}$ for all $\phi_m$, to zeroth order in $2\pi L_s i_c/\phi_o$. Thus the fluctuations of the SQUID ring are equivalent to an uncertainty in $\phi_{xm}$ of spectral density.

11) $$\langle\delta\phi_{xm}^2(\nu)\rangle^{\frac{1}{2}} = (4k_B T_s/R_s)^{\frac{1}{2}} .$$

Combining Eq. (10) with either Eq. (8) or Eq. (9), depending on whether the SQUID system is sensitive to the SQUID ring response at frequency $\omega$ or to the peak response, the maximum SQUID sensitivity or the minimum observable flux signal is

12) $$\delta\phi_{x,min}^{(dc)} \simeq \frac{\phi_o}{2\pi L_s i_c 2J_{1,m}}\left(\frac{4k_B T_s L_s^2 \Delta f}{R_s}\right)^{\frac{1}{2}}$$
$$\simeq \frac{\phi_o}{2\pi L_s i_c}\left(\frac{4k_B T_s L_s^2 \Delta f}{R_s}\right)^{\frac{1}{2}} ,$$

where $\Delta f$ is the post-detection bandwidth of the SQUID system. This result was originally obtained by Danilov and Likharev[14] in their analysis of the limiting characteristics of the low critical current SQUID.

### III.2. $L_s i_c \lesssim \phi_o/2\pi$

For larger values of critical current the fluctuation amplitude of $\phi$ is no longer independent of $\phi$ and $\phi_x$. In the usual case of $L_s k_B T_s/\phi_o^2 << 1$ these fluctuations can still be treated however as small excursions about the minimum of the potential $U(\phi,\phi_x)$. Therefore the spectral density of the fluctuations in $\phi$ is given by

$$13) \quad \langle \delta^2\phi(\nu)\rangle^{\frac{1}{2}} = L_s[1 + (2\pi L_s i_c/\phi_o)\cos 2\pi\phi/\phi_o]^{-1}(4k_B T_s/R_s)^{\frac{1}{2}} \quad ,$$

a quantity that depends directly on the internal flux $\phi$ and hence on the applied flux $\phi_x$. As a result the uncertainty in the amplitude of the internal flux response $\phi_m$ depends on the position of the SQUID ring on the $\phi_m$-$\phi_{xm}$ response curve. This can be clearly seen in Fig. 8 where $\phi_m$-$\phi_{xm}$ response curves as calculated numerically from Eq. (1), with a noise current term included, are shown for various values of $L_s i_c$. In all cases the external flux amplitude $\phi_{xm}$ is increased sufficiently rapidly in the calculation so that fluctuations in $\phi_m$ are not averaged out on the scale of the drawing. The correlation between the fluctuation amplitude and the slope of the response curve is apparent. In general the spectral density of the fluctuations in $\phi_m$ is given, at least approximately by

$$14) \quad \langle \delta\phi_m^2(\nu)\rangle^{\frac{1}{2}} \simeq L_s(d\phi_m/d\phi_{xm})(4k_B T_s/R_s)^{\frac{1}{2}} \quad .$$

Since during rf SQUID operation the ring is biased on a region of maximum slope on the $\phi_m$-$\phi_{xm}$ response curve, it is the maximum amplitude of this spectral density that must be considered

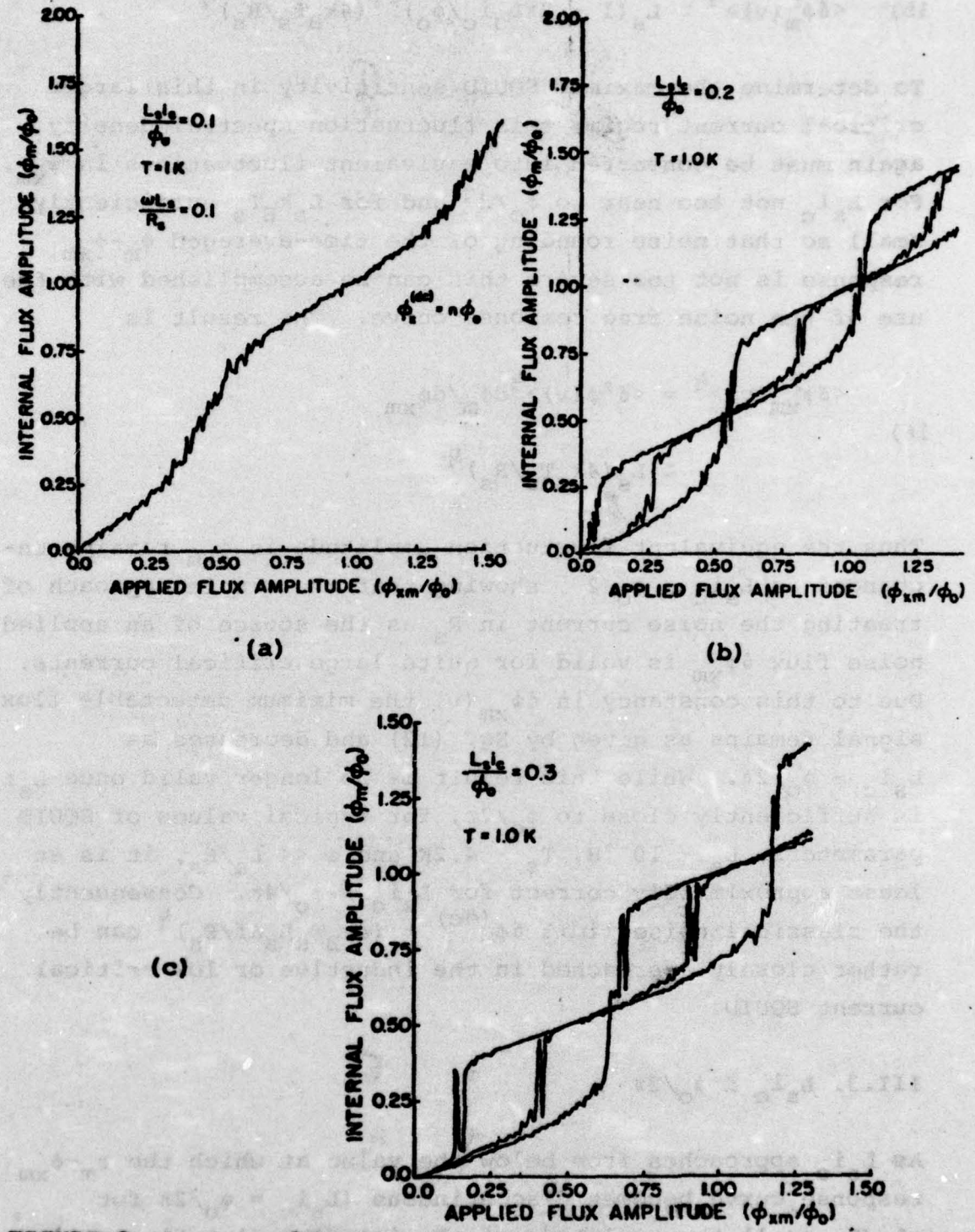


FIGURE 8. $\phi_m$-$\phi_{xm}$ rf response curve calculated numerically from a noise term included vor various values of $L_s i_c$. Again the drive frequency $\omega \approx 0.1 R_s/L_s$. For clarity only the curve for $\phi_x^{(dc)} = n\phi_o$ is shown in (a). The simulation assumes $T_s$ = 1K and $L_s = 10^{-9}$H.

$$15) \quad \langle \delta\phi_m^2(\nu) \rangle^{\frac{1}{2}} \approx L_s (1 - 2\pi L_s i_c/\phi_o)^{-1} (4k_B T_s/R_s)^{\frac{1}{2}} \quad .$$

To determine the maximum SQUID sensitivity in this larger critical current regime this fluctuation spectral density again must be converted into equivalent fluctuations in $\phi_{xm}$. For $L_s i_c$ not too near to $\phi_o/2$ and for $L_s k_B T_s$ sufficiently small so that noise rounding of the time-averaged $\phi_m - \phi_{xm}$ response is not too severe this can be accomplished with the use of the noise free response curve. The result is

$$16) \quad \begin{aligned} \langle \delta\phi_{xm}^2(\nu) \rangle^{\frac{1}{2}} &= \langle \delta^2\phi(\nu) \rangle^{\frac{1}{2}} d\phi_m/d\phi_{xm} \\ &\approx L_s (4k_B T_s/R_s)^{\frac{1}{2}} \quad . \end{aligned}$$

Thus the equivalent fluctuation amplitude in $\phi_{xm}$ remains unchanged as $L_s i_c \to \phi_o/2$ , showing that the simple approach of treating the noise current in $R_s$ as the source of an applied noise flux $\delta\phi_{xm}$ is valid for quite large critical currents. Due to this constancy in $\delta\phi_{xm}(\nu)$ the minimum detectable flux signal remains as given by Eq. (12) and decreases as $L_s i_c \to \phi_o/2\pi$. While this result is no longer valid once $L_s i_c$ is sufficiently close to $\phi_o/2\pi$, for typical values of SQUID parameters, $L_s \sim 10^{-9}$H, $T_s \sim 4.2$K and $\omega \ll L_s/R_s$, it is at least approximately correct for $L_s i_c \leq \phi_o/4\pi$. Consequently the classical noise limit $\delta\phi_x^{(dc)} \approx (4k_B T_s L_s \Delta f/R_s)^{\frac{1}{2}}$ can be rather closely approached in the inductive or low critical current SQUID.

### III.3. $L_s i_c \geq \phi_o/2\pi$

As $L_s i_c$ approaches from below the value at which the $\phi_m - \phi_{xm}$ response curve becomes discontinuous ($L_s i_c = \phi_o/2\pi$ for $\omega L_s/R_s \ll 1$) the amplitude of the internal flux fluctuations, when the ring is biased on a region of maximum slope of the response curve, eventually increases sufficiently that the intrinsic noise calculation can no longer be treated as a

problem of classical fluctuations. Instead it must be treated as a problem of random transitions between quantum states. This effect can be seen in Fig. 8 and it commences somewhere below $L_s i_c = \phi_o/2\pi$ at a point dependent on $(L_s k_B T_s)^{\frac{1}{2}}$.

When the SQUID ring is biased at or near the region of maximum slope of the $\phi_m$-$\phi_{xm}$ response curve, at the peak of the rf cycle the internal flux $\phi$ fluctuates back and forth between the two accessible states at a frequency which is much greater than the bias frequency $\omega$, assuming $\omega << R_s/L_s$. This results in an uncertainty in the peak response $\phi_m$ which depends on the fluctuation frequency. As $L_s i_c$ exceeds $\phi_o/2\pi$ the probability of reverse transition diminishes and eventually at most only one forward transition in $\phi$ can be made at the peak of every half rf cycle. As a result of this pronounced decrease in the fluctuation frequency the minimum detectable flux of the rf SQUID increases until the maximum SQUID sensitivity reaches the value calculated by Kurkijärvi and Webb[15] for $L_s i_c >> \phi_o/2\pi$.

As an alternative to the exact calculation of Kurkijärvi and Webb the minimum detectable flux in the large critical current regime can be discussed along lines similar to those used here for the case $L_s i_c < \phi_o/2\pi$. Assuming $L_s i_c$ is sufficiently large and $\phi_x^{(dc)} = n\phi_o$, the peak amplitude $\phi_m$ of the rf response to $\phi_x$ is either ~0 or $\phi_o$ during any rf cycle, depending on whether or not a transition occurs during the peak of that cycle. If the probability that such a transition occurs every cycle is p, where p depends on the value of $\phi_{xm}$, then the average value of the internal flux response is simply

$$17) \quad \langle \phi_m \rangle = p\phi_o \quad ,$$

and for frequencies much less than $\omega$ the spectral density of the fluctuations in $\phi_m$ is

$$18) \quad \langle \delta\phi_m^2(\nu) \rangle^{\frac{1}{2}} = [p(1-p)]^{\frac{1}{2}} \phi_o (2\pi/\omega)^{\frac{1}{2}} \quad .$$

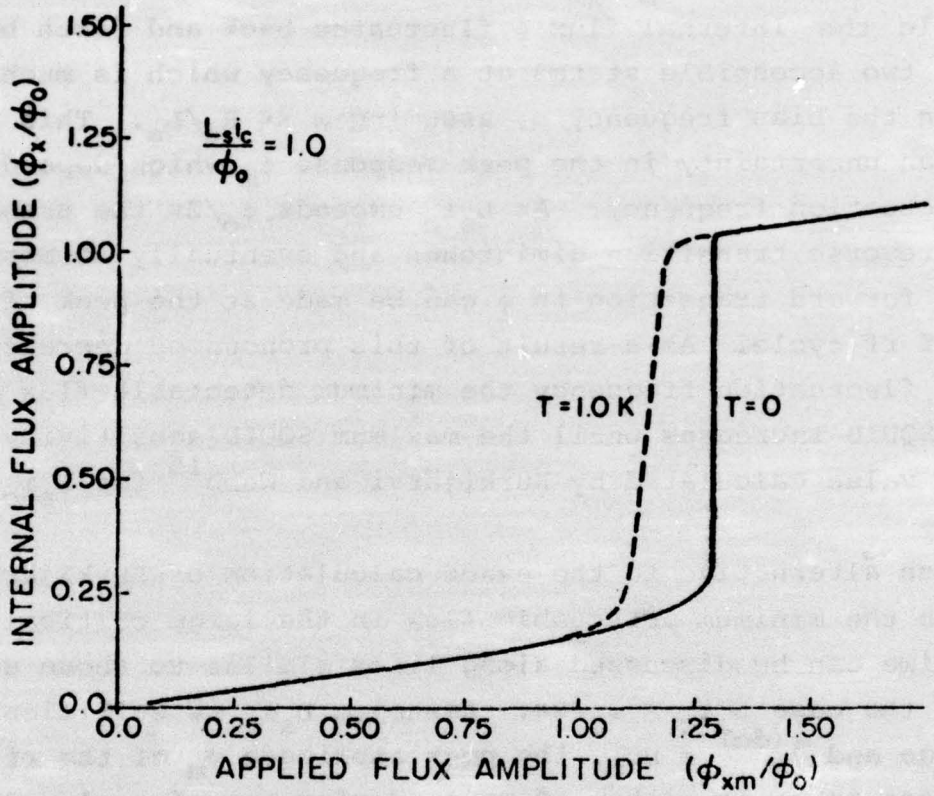


FIGURE 9. A numerically calculated time averaged rf response curve for the case where T = 0 and T = 1.0K. The slope of the dotted curve in the T = 1.0K case is equal to the fluxoid transition uncertainty as calculated by Kurkijärvi and Webb.

To convert these fluctuations in $\phi_m$ into equivalent fluctuations in $\phi_{xm}$ it is necessary to use the $\phi_m$-$\phi_{xm}$ response curve which has been time-averaged over a period >> $1/\omega$. An example of such a time averaged response curve is shown in Fig. 9. The effect of the averaging is to remove the discontinuity from the response curve, replacing it with a curve of finite slope which is centered at a point on the $\phi_{xm}$ axis somewhat to the left of the discontinuity in the noise-free case. (In general the amount of shift depends upon $i_s$, $T_s$ and $\omega$.[8]) This curve, which is basically a straight line segment over most of its length represents the probability that a fluxoid transition will occur once every cycle for a particular value of $\phi_{xm}$. The slope of the curve $d\phi_m/d\phi_{xm}$ is then simply the inverse of the width of the fluxoid transition uncertainty as calculated by Kurkijärvi.[8] Thus the equivalent spectral density of fluctuations in $\phi_{xm}$ where the SQUID ring is biased on the region of maximum slope of the time-averaged response curve is

$$19) \quad \langle \delta\phi^2_{xm}(\nu) \rangle^{1/2} \approx [p(1-p)]^{1/2} (2\pi/\omega)^{1/2} \sigma$$

where $\sigma \approx L_s i_c (k_B T_s 2\pi/\phi_o i_c)^{2/3}$ .

This approximate result is of course only valid for biasing near the center of the region of maximum slope of the response curve where $p \approx 0.5$. In this case the limiting sensitivity is

$$20) \quad \delta\phi^{(dc)}_{x,min} \approx 0.5 \left(\frac{2\pi\Delta f}{\omega}\right)^{1/2} L_s i_c \left(\frac{2\pi k_B T_s}{\phi_o i_c}\right)^{2/3} ,$$

which is essentially the result of K-W.

The limiting intrinsic noise for an rf SQUID is thus a minimum for $i_c$ slightly less than the value required for the $\phi_m$-$\phi_{xm}$ response curve to become discontinuous, which is $2\pi L_s i_c/\phi_o = 1$ for $\omega L_s/R_s << 1$. As $i_c$ increases above this value the

intrinsic noise increases rather rapidly toward the limit calculated by K-W for $L_s i_c >> \phi_o/2\pi$. This is not the case however when the bias frequency is increased so that $\omega L_s/R_s \to 1$. For $\omega L_s/R_s \gtrsim 1$ it is straightforward to show that the intrinsic noise for the case of both a continuous and discontinuous response curve can very closely approach the limiting classical value. Therefore for low frequency operation $\omega L_s/R_s << 1$, if the intrinsic noise is of practical importance, which to date is seldom the case, then $i_c$ should be adjusted so that $L_s i_c \lesssim \phi_o/2\pi$. For higher frequencies this constraint is largely removed.

## IV. CIRCUIT CONSIDERATIONS

In the usual case, the rf SQUID circuit consists of a current-driven high Q tank circuit of inductance $L_t$ and capacitance $C_t$. The circuit is inductively coupled to the SQUID ring through mutual inductance M and the circuit is driven at or near its resonant frequency $\omega_o$. When suitably biased and tuned, the tank circuit voltage is periodically modulated by $\delta\phi_x^{(ac)}$, yielding the SQUID signal. A schematic representation of such a SQUID circuit is shown in Fig. 10. The details of the tank circuit response in both the low critical current[4,10-14] and high critical current[4,6,9] regimes have been extensively discussed in the literature. Here only a few basic features will be sketched so as to establish a qualitative picture of the various noise sources and optimum coupling conditions for the rf SQUID

### IV.1. rf I-V Characteristic

In general terms, the rf tank circuit is driven at a frequency $\omega$ such that changes of the rf flux amplitude within the SQUID ring present maximum opposition to change in the applied flux. As discussed by Ramsma and others[10-14] in the very low critical current regime where the flux response at frequency $\omega$

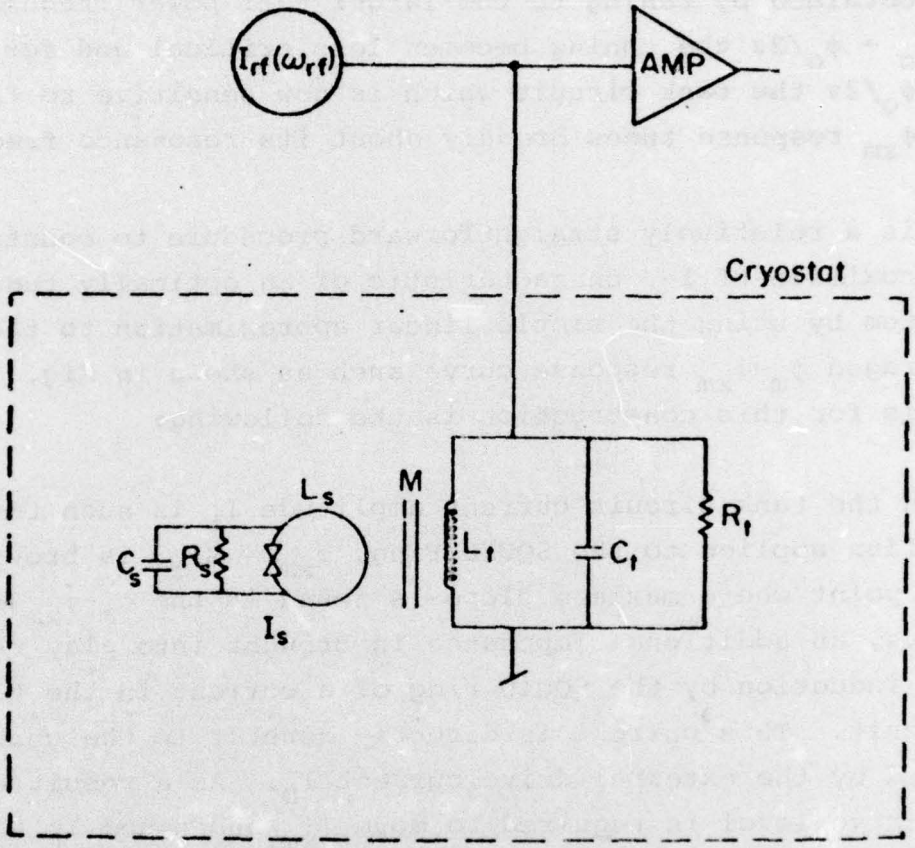


FIGURE 10. Schematic representation of a standard rf SQUID system.

is in phase with the drive flux this requires that the biasing frequencies to be either of the half power frequencies of the resonant circuit. For larger values of $i_c$ when screening currents in the SQUID ring become important the circuit response is no longer anti-symmetric about $\omega_o$ and maximum signal is obtained by tuning to the larger half power frequency. As $L_s i_c \to \phi_o/2\pi$ the tuning becomes less critical and for $L_s i_c >> \phi_o/2\pi$ the tank circuit which is now sensitive to the peak $\phi_m$-$\phi_{xm}$ response tunes broadly about its resonance frequency $\omega_o$.

It is a relatively straightforward procedure to construct an approximate rf I-V characteristic of an optimally tuned SQUID system by using the simple linear approximation to the time-averaged $\phi_m$-$\phi_{xm}$ response curve such as shown in Fig. 7. The basis for this construction is the following:

When the tank circuit current amplitude $I_t$ is such that the rf flux applied to the SQUID ring, $\phi_{xm} = MI_t$, is brought to the point where maximum slope is found in the $\phi_m$-$\phi_{xm}$ response curve, an additional impedance is brought into play through the induction by the SQUID ring of a current in the tank circuit. This current is directly counter to the current induced by the external drive current $I_D$. As a result a greater rf drive level is required to move $\phi_{xm}$ and hence $I_t$ through the region of steepest slope in the $\phi_m$-$\phi_{xm}$ response curve than through the region of minimum slope. Consequently a "step" is created in the rf I-V characteristic since the tank circuit voltage $V_t = \omega L_t = \omega L_t \phi_{xm}/M$. The length of this step in terms of the external drive current $I_D$ is, to a fair approximation,

$$21) \quad I_{D,step} \simeq \frac{M}{L_t L_s} \Delta\phi_m + \frac{1}{MQ} \Delta\phi_{xm} \quad ,$$

where $\Delta\phi_m$ and $\Delta\phi_{xm}$ are the extent in $\phi_m$ and $\phi_{xm}$, respectively, covered by the steeper straight line segments of the response curve. (See Fig. 7.) In the low critical current regime, as in Fig. 7, we have $\Delta\phi_m/\Delta\phi_{xm} = (1 - 2\pi L_s i_c/\phi_o)^{-1}$, although to be

accurate the harmonic response function should be employed for which $\Delta\phi_m/\Delta\phi_{xm} = [(1 - 2L_s i_c J'_{1,m})(2\pi\phi_m/\phi_o)]^{-1}$ gives the slope of the first straight line segment of the approximate response curve. For $L_s i_c > \phi_o/2\pi$, $\Delta\phi_{xm}/\Delta\phi_{xm}$ is the reduced fluxoid transition uncertainty $\sigma/\phi_o$. The rf voltage change along the step is, of course,

$$22) \quad V_{t,\,step} \approx \frac{\omega L_t}{M} \Delta\phi_{xm} \quad .$$

The various steps in the rf I-V characteristic are separated by "risers". The length of these risers in $I_D$ can be estimated from the fact that from the end of one full step to the beginning of another $I_D$ must increase by a minimum amount

$$23) \quad I_{D,riser} \approx \frac{1}{MQ} (\phi_o - \Delta\phi_{xm}) \quad ,$$

while the tank circuit voltage changes by an amount

$$24) \quad V_{t,riser} \approx \frac{\omega L_t}{M} (\phi_o - \Delta\phi_{xm}) \quad .$$

By determining the changes in position of the various steps and risers on the rf I-V characteristic as $\phi_x^{(dc)}$ varies, it is quickly found that the voltage modulation by the applied flux signal $\delta\phi_x^{(dc)}$ of the positions of the rf steps at constant rf drive level is

$$\delta V_t(\delta\phi_x^{(dc)}) \approx \frac{\omega L_t}{M} (1 - \Delta\phi_{xm}/\Delta\phi_m)\, \delta\phi_x^{(dc)} \quad , \quad \delta\phi_x^{(dc)} < \phi_o/2$$

or

$$\delta V_t \approx \frac{\omega L_t}{M}\left(\frac{2\pi L_s i_c}{\phi_o}\right) \delta\phi_x^{(dc)} \quad , \quad 2\pi L_s i_c/\phi_o \leq 0.5$$

$$25) \quad \delta V_t \approx \frac{\omega L_t}{M} (1 - \sigma/\phi_o)\, \delta\phi_x^{(dc)} \quad , \quad 2\pi L_s i_c/\phi_o > 1 \quad .$$

While Eqs. (20)-(25) are clearly only approximate, particularly for the low critical current case, they can be used to

construct rf I-V characteristics which agree reasonably well with I-V's which we have obtained from complete digital simulations of rf SQUIDs. Examples of such I-V's are shown in Figs. 11 and 12 for both the low critical current and high critical current cases. In all the I-V's shown the drive frequency is at or close to its optimum value. In general it is found from the simulations that the values of the maximum dc flux modulation amplitude and of the step and riser lengths are, at least for the first step, well within a factor of two of the values given above, once corrections have been made for the relatively large bias frequencies that were necessary in the simulations.

A rather important result, that can be extracted from either the arguments given above or directly from the simulations, is that the inductive SQUID, where $2\pi L_s i_c/\phi_o < 1$, can yield a signal that is within a factor of two of the maximum that is obtainable from the higher critical current device. Thus if intrinsic noise does become a practical problem, it might be appropriate for the critical current to be reduced from its usual value, $L_s i_c \sim \phi_o$, to $L_s i_c \simeq 0.5\phi_o/2\pi$, where the intrinsic noise is considerably less, assuming $\omega << R_s/L_s$.

## IV.2. Circuit Noise and Optimum Coupling

In general there are three independent noise sources in an rf SQUID — the rf amplifier, the tank circuit, and the SQUID ring itself. Kurkijärvi[16] has analyzed the problem of tank circuit noise for the case of the large critical current device. Using the arguments given in the previous section, his results can be readily generalized to cover the lower critical current case.

The essential point of Kurkijärvi's analysis is that the amplitude of the tank circuit voltage fluctuations is determined by the bias position on the rf I-V characteristic; that is,

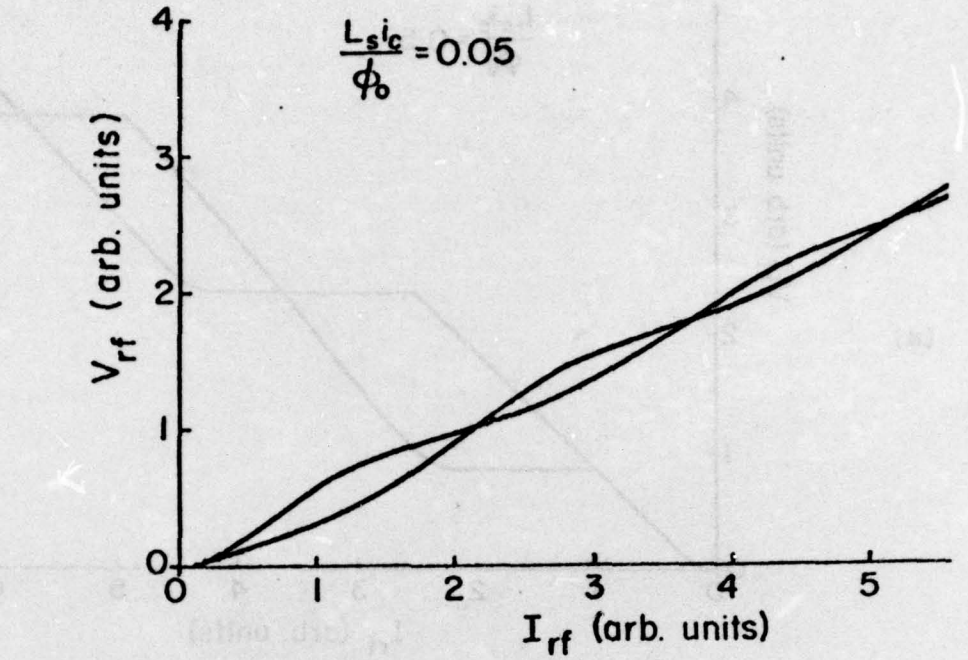


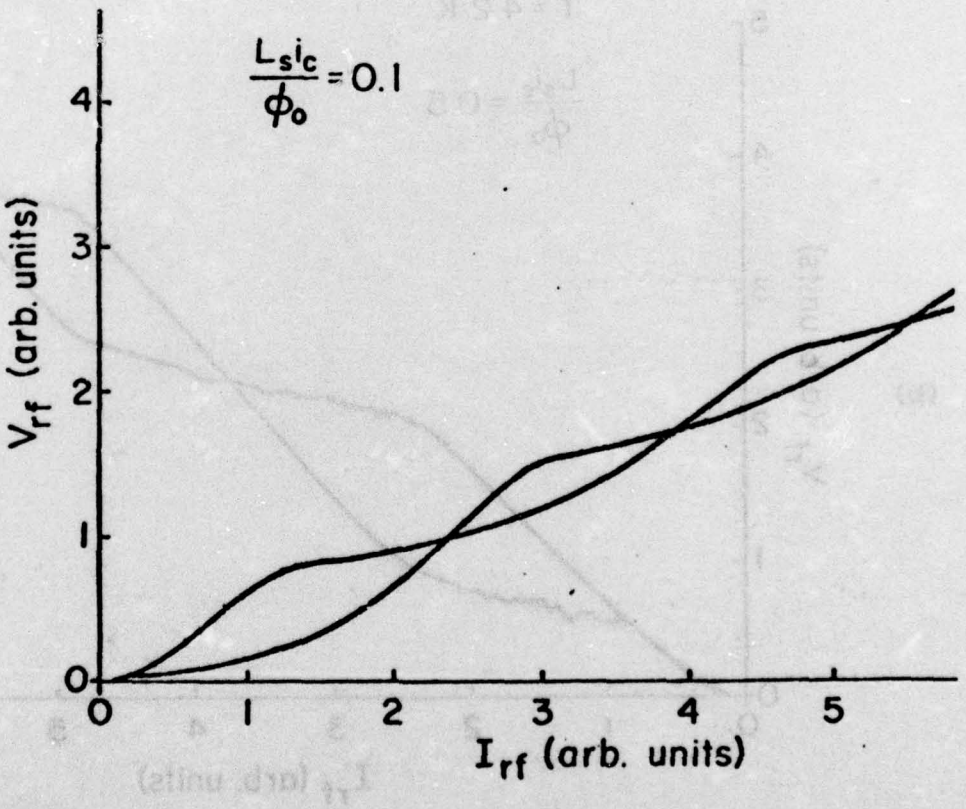


FIGURE 11. Simulated rf I-V characteristics for the low critical current SQUID. In the simulations $\omega L_s R_s = 0.1$, $K^2Q = 4$. The tuning is close to optimum.

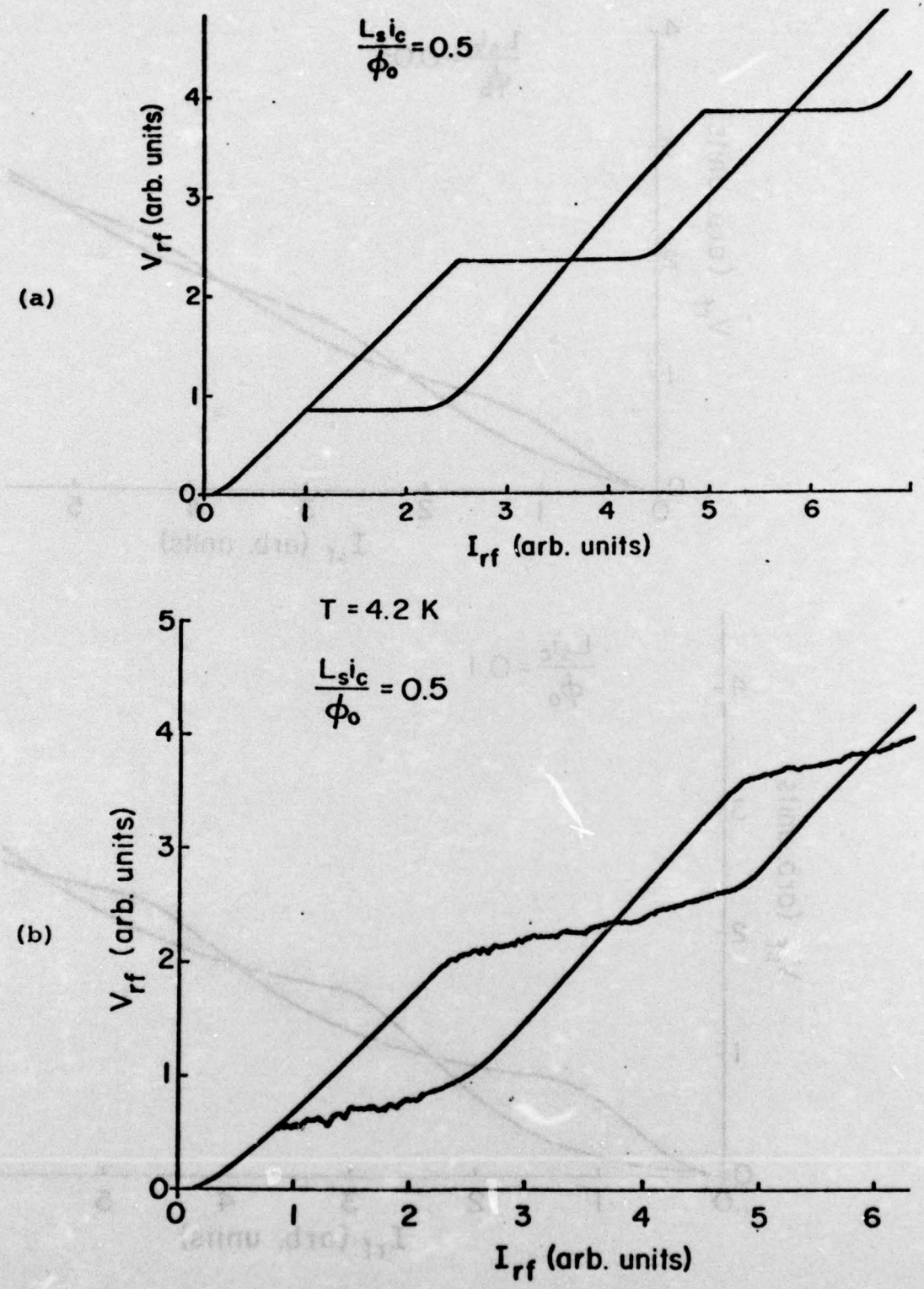


FIGURE 12. Simulated rf I-V characteristic for $L_s i_c = 0.5\phi_o$. In (a) T = 0; (b) T = 4.2K. $K^2Q = 1$ and the voltage scale is the same as in Fig. 11.

the origin of tank circuit noise is the current fluctuations in the equivalent tank circuit shunt resistor $R_t$. The response of the circuit to these fluctuations is determined by the local tank circuit impedance $dV_t/dI_D$. Since during SQUID operation the system is biased on an rf step, the tank circuit voltage fluctuation spectral density is

$$\langle \delta V_T^2(\nu) \rangle^{\frac{1}{2}} = \frac{dV_{t,step}}{dI_{D,step}} \left( \frac{4k_B T_t}{Q\omega L_t} \right)^{\frac{1}{2}}$$

or

$$26) \quad \langle \delta V_T^2(\nu) \rangle^{\frac{1}{2}} = \frac{\Delta\phi_{xm}}{\Delta\phi_{xm} + K^2 Q \Delta\phi_m} \left( 4k_B T_t Q\omega L_t \right)^{\frac{1}{2}}$$

where $K^2 = M^2/L_s L_t$ and is the coupling constant between the SQUID ring and $L_t$. Now as $2\pi L_s i_c/\phi_o$ increases from zero to greater than one, $\Delta\phi_{xm}$ decreases from $\phi_o/2$ to its limiting value $\sigma/\phi_o$ while $\Delta\phi_m$ increases from $\phi_o/2$ to $\phi_o$. Thus in the limit of large critical current, Eq. (26) reduces to the Kurkijärvi result.[7,16] Provided the critical current is not too small, $2\pi L_s i_c/\phi_o \gtrsim \frac{1}{4}$ and that $K^2 Q \gtrsim 1$, Eq. (26) can be approximated by

$$27) \quad \langle \delta V_T^2(\nu) \rangle^{\frac{1}{2}} \approx \frac{(\Delta\phi_{xm}/\Delta\phi_m)}{K^2 Q} \left( 4k_B T_t Q\omega L_t \right)^{\frac{1}{2}} ,$$

where $\Delta\phi_{xm}/\Delta\phi_m \approx 1 - 2\pi L_s i_c/\phi_o$ for small $i_c$ and $\Delta\phi_{xm}/\Delta\phi_m \approx \sigma/\phi_o$ for $L_s i_c >> \phi/2\pi$.

With this result the total equivalent noise power spectral density for the rf SQUID can be written as

$$\langle \delta\phi_N^2(\nu) \rangle = \frac{K^2 L_s}{\omega^2 L_t} \frac{\langle V_A^2(\nu) \rangle}{(1 - \Delta\phi_{xm}/\Delta\phi_m)} + \frac{(\Delta\phi_{xm}/\Delta\phi_m)^2}{(1 - \Delta\phi_{xm}/\Delta\phi_m)^2}$$

$$28) \quad \times \left[ \frac{k_B T_t L_s}{\omega} \frac{1}{K^2 Q} \right] + \langle \delta\phi_i^2(\nu) \rangle ,$$

where $\langle \delta V_A^2(\nu) \rangle^{\frac{1}{2}}$ = spectral density of the voltage noise in the amplifier and where the intrinsic flux noise spectral density $\langle \delta \phi_i^2(\nu) \rangle^{\frac{1}{2}}$ is

$$\langle \delta \phi_i^2(\nu) \rangle^{\frac{1}{2}} \approx \frac{2\pi L_s i_c}{\phi_o} \left( \frac{4 k_B T_s L_s}{R_s} \right)^{\frac{1}{2}} , \quad L_s i_c < \phi_o/2\pi$$

29)

$$\approx \frac{1}{1 - \sigma/\phi_o} \left( \frac{0.5\pi}{\omega} \right)^{\frac{1}{2}} \sigma , \quad L_s i_c >> \phi_o/2\pi \quad .$$

Since the effective tank circuit noise temperature $T_t$ is usually greater than, and certainly never less than, $T_s$, Eqs. (28) and (29) show that for the inductive SQUID with coupling $K^2Q \sim 1$ the tank circuit noise term will invariably be larger than the intrinsic noise term provided $\omega << R_s/L_s$. Only for the impractical case of tight coupling does the tank circuit noise term approach the intrinsic noise level, which however is quite small. For the larger critical current case the intrinsic noise is greater and the ranking between the two terms depends on whether the ratio $L_s k_B T_t / \phi_o K Q \lesssim \pi/2$.

In most practical SQUID systems the amplifier noise term dominates. To minimize this noise the coupling constant K is reduced to some minimum value. Usually this value is set by the requirement that, to obtain a continuous modulation of the step voltage by $\delta\phi_x^{(dc)}$, it is necessary that $I_{D,step} \gtrsim I_{D,riser}$. For $L_s i_c \gtrsim \phi_o/2\pi$ this requires that $K^2Q \gtrsim 1$, to within the accuracy of the approximations employed here. For $L_s i_c \lesssim 0.5\phi_o/2\pi$ the extensive rounding in the actual rf I-V characteristic which is not accounted for in the approximations used here require $K^2Q$ to be somewhat greater than unity for maximum modulation of $V_t$ by a flux change $\delta\phi_x^{(dc)} = \phi_o/2$.

The constraint $K^2Q \gtrsim 1$ is not rigorous and it is possible to increase the SQUID signal for small flux changes $\delta\phi_x^{(dc)} < \phi_o/2$ by decoupling beyond $K^2Q = 1$. This is most effective in the

larger critical current regime. The range of $\delta\phi_x^{(dc)}$ for which the tank circuit voltage is responsive decreases as $\sim 1/K^2$. Still, some increase in the small signal response beyond the value

$$\delta V_t \approx \omega (QL_t/L_s)^{\frac{1}{2}} (1 - \Delta\phi_{xm}/\Delta\phi_m)\, \delta\phi_x^{(dc)}$$

is possible.

In some cases decoupling of the SQUID ring even to the point $K^2Q \approx 1$ may not be desirable as the tank circuit noise increases as $(K^2Q)^{-1}$. The ratio of the amplifier noise term to tank circuit noise term is

$$30) \quad \frac{\langle \delta V_A^2(\nu)\rangle^{\frac{1}{2}}}{\langle \delta V_T^2(\nu)\rangle^{\frac{1}{2}}} \approx \frac{K^2Q \langle \delta V_A^2(\nu)\rangle^{\frac{1}{2}}}{(Q\omega L_t k_B T_t)^{\frac{1}{2}}} \left(\frac{\Delta\phi_m}{\Delta\phi_{xm}}\right) .$$

Since the maximum value of $\Delta\phi_m/\Delta\phi_{xm}$ is $\lesssim 10$ for typical SQUID parameters, for sufficiently high tank circuit impedance the tank circuit noise may become a factor as improvements in rf amplifiers continue to be made. In this case tighter coupling than $K^2Q = 1$ may be required for maximum sensitivity.

## V. WEAK LINK EFFECTS AND ULTIMATE SENSITIVITY

Only the case of a sinusoidal current-phase relation for the weak link has been considered. In practice, weak links that are employed in SQUIDs often have distinctly non-sinusoidal current-phase relations. A typical non-sinusoidal current-phase relation is shown in Fig. 13. The result of such departures from ideal behavior is not drastic but it is detrimental to SQUID sensitivity.

The major effect of non-sinusoidal current-phase relations is to reduce the maximum signal amplitude that can be extracted from a SQUID system. As the critical phase angle $\theta_c$ of the current-phase relation increases beyond the optimum $\pi/2$ value

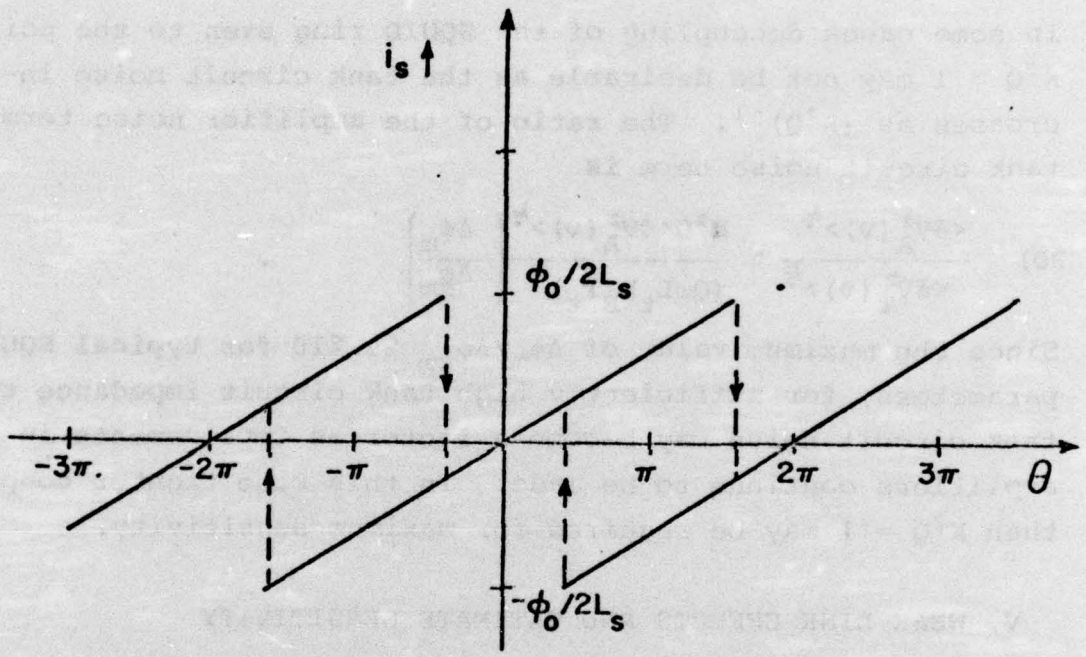


FIGURE 13. The measured non-sinusoidal current phase relation of a 1μ square tin microbridge.

the effect is to decrease the amplitude of $\Delta\phi_m$ on the steeper parts of the rf $\phi$-$\phi_x$ response curve. In the low critical current regime the result is a corresponding increase in the minimum coupling constraint on $K^2Q$. For $\theta_c \gtrsim \pi$ the SQUID can only be operated in the discontinuous or hysteretic mode which has the higher intrinsic noise amplitude. Even then the minimum coupling constraint $I_{step} \gtrsim I_{riser}$ acts to decrease the available SQUID signal. In addition it has been found[7] that the fluxoid transition uncertainty also increases with critical phase angle $\theta_c$. Besides increasing the intrinsic noise amplitude directly, this imposes a greater lower bound on the magnitude of $\Delta\phi_{xm}/\Delta\phi_m$. This results in turn in larger tank circuit noise and, if the transition uncertainty $\sigma \gtrsim 0.3\phi_o$, in a direct decrease in maximum signal strength. Experimentally[17] it has been found that even for extremely non-sinusoidal current-phase relations the transition uncertainty $\sigma$ seldom increases beyond a factor of 5 of the value for a sinusoidal current-phase relation. It appears that local inhomogeneities in the larger weak links which have the non-sinusoidal relations restrict the fluctuations in the weak link. Consequently, practically any weak link which has sufficiently small critical current $i_c \simeq \phi_o/L_s$ can be used in an rf SQUID in the discontinuous mode. While the performance is degraded if $\theta_c >> \pi/2$ a usable signal can in fact usually be obtained, provided the link is underdamped and $\omega$ is not too large.

Finally it is interesting, although perhaps academic at present, to determine what the ultimate intrinsic SQUID sensitivity might be. It has been shown that in general when discussing SQUID sensitivity the appropriate sensitivity figure is not the total equivalent flux noise spectral density $\langle\delta\phi_N^2(\nu)\rangle^{\frac{1}{2}}$ but rather one which takes into account the efficiency by which flux signals can be coupled into the SQUID ring. In this case the SQUID sensitivity can be expressed in terms of an energy resolution $\delta E$ where $\delta E(\nu) \simeq \langle\delta\phi_N^2(\nu)\rangle/K'L_s$ where $K'$ is the coupling constant between a signal coil and the

SQUID ring. Assuming that K' can be set to ≈1 for the most favorable case of $L_s i_c \lesssim \phi_o/2\pi$, the result is

31) $\delta E(\nu) \approx 4k_B T_s L_s/R_s$ .

For an ideal Josephson junction $R_s \approx \pi\Delta(0)/2ei_c$ where $\Delta(0) = 1.76k_B T_c$ and is the T = 0 energy gap of the superconductor and where the temperature $T_s$ of the weak link is assumed to be $<<T_c$ of the superconducting material. In this case we have

32) $$\delta E(\nu) \approx \frac{4k_B T_s L_s (2ei_c)}{1.76\pi k_B T_c}$$

but $L_s i_c \approx \phi_o/2\pi = \frac{h}{4\pi e}$, so

33) $$\delta E(\nu) \approx \frac{4T_s}{1.76\pi T_c}\frac{h}{2\pi}$$ .

Thus for any rf SQUID system which has an ideal Josephson junction for the weak link, fabricated from any superconductor, and which is operated at $T_s \lesssim 0.5T_c$ the minimum intrinsic energy resolution is simply due to the zero point oscillations as set by the uncertainty principle:

34) $$\frac{\langle\delta\phi_N^2(\nu)\rangle}{L_s} \gtrsim h \approx 6.6\times10^{-34} \text{ Joules/Hz}$$ .

In terms of magnetic flux for a typical ring inductance $L_s \approx 10^{-9}$H this corresponds to an ultimate flux sensitivity

35) $\langle\delta\phi_N^2(\nu)\rangle^{\frac{1}{2}} \gtrsim 4\times10^{-7}\phi_o/\sqrt{\text{Hz}}$ ,

which is somewhat more than a factor of ten lower than the best sensitivity that has ever been achieved in practice,[19] to the knowledge of this author. It would be rather impressive if this limiting noise figure is in fact ever closely approached.

This research supported by the Office of Naval Research. I am happy to acknowledge the very extensive and essential contributions of Dr. L. D. Jackel to the work presented here.

References

1. A. H. Silver and J. E. Zimmerman: Phys. Rev. 157, 317 (1967).
2. W. W. Webb: IEEE Trans. Magn. 8, 51 (1972).
3. J. M. Goodkind and D. L. Stolfa: Rev. Sci. Instrum. 41, 799 (1970).
4. J. Clarke: Proc. IEEE 61, 8 (1973).
5. R. P. Giffard, R. A. Webb and J. C. Wheatley: J. Low Temp. Phys. 6, 533 (1972).
6. J. E. Zimmerman: Cryogenics 12, 19 (1972).
7. L. D. Jackel and R. A. Buhrman: J. Low Temp. Phys. 19, 201 (1975).
8. J. Kurkijärvi: Phys. Rev. B 6, 832 (1972).
9. R. A. Buhrman and L. D. Jackel: IEEE Trans. Magn., in press.
10. P. K. Hansma: J. Appl. Phys. 44, 4191 (1973).
11. O. H. Soerensen, unpublished.
12. S. N. Erne, H. D. Hahlbohm and H. Lübbig: J. Appl. Phys.,
13. R. Rifkin, D. A. Vincent, B. S. Deaver and P. K. Hansma: J. Appl. Phys. 47, 2645 (1976).
14. V. V. Danilov and K. K. Likharev: Sov. Phys.-Tech. Phys. 20, 697 (1976).
15. J. Kurkijärvi and W. W. Webb: IEEE Pub. No. 72CHO682-5-TABSC (IEEE, New York, 1972), p. 581.
16. J. Kurkijärvi: J. Appl. Phys. 44, 3729 (1973).
17. L. D. Jackel and R. A. Buhrman: unpublished.
18. J. H. Claassen: J. Appl. Phys. 46, 2268 (1975).
19. M. R. Gaerttner operating at 440 MHz with a cooled preamplifier has obtained an equivalent flux noise spectral density $\langle \delta\phi_N^2(\nu) \rangle^{\frac{1}{2}} \simeq 7\times10^{-6}\phi_o/\mathrm{Hz}^{\frac{1}{2}}$ with a toroidal point contact device having $L_s \simeq 1\times10^{-9}$H.